Improved Multi-band Transfer Matrix Method for Calculating Eigenvalues and Eigenfunctions of Quantum Well and Superlattice Structures

Byoung-Whi Kim, Yong Il Jun, and Hee Bum Jung

CONTENTS

ABSTRACT

We present an improved transfer matrix algorithm which can be used in solving general n-band effective-mass Schrödinger equation for quantum well structures with arbitrary shaped potential profiles (where n specifies the number of bands explicitly included in the effective-mass equation). In the proposed algorithm, specific formulas are presented for the three-band (the conduction band and the two heavy- and light-hole bands) and two-band (the heavy- and light-hole bands) effective-mass eigensystems. Advantages of the present method can be taken in its simple and unified treatment for general $n \times n$ matrix envelope-function equations, which requires relatively smaller computation efforts as compared with existing methods of similar kind. As an illustration of application of the method, numerical computations are performed for a single GaAs/AlGaAs quantum well using both the two-band and three-band formulas. The results are compared with those obtained by the conventional variational procedure to assess the validity of the method.

I. INTRODUCTION

As the ability of tailoring the electronic band structure of semiconductor quantum wells (QWs) and superlattices (SLs) according to controlled variations in the growth parameters has increased, the novel electronic and optical properties of heterostructure systems have led to intensive research activities to exploit the use of such systems in various technological areas including semiconductor lasers, electro-optical modulators, infrared detectors, giant quantum wells, etc. [1]-[14]. In order to understand the features exhibited in the electronic characteristics and optical spectra of these heterojunction structures, it becomes essential to improve the calculation of their electronic band structure. The tight-binding [15] and envelope-function (effective-mass) [16] approximations have been widely used for such calculations.

In the effective-mass approximation, various computation methods [17]-[30] have been developed and used for the calculations. The variational procedure has been extensively used and proven to be an excellent tool for such calculations [20]-[26]. However, although this method can take into account differences in band parameters between different material layers [20], [21], it requires relatively large amount of computing time to perform numerical computations for multiband effective-mass eigensystems.

The transfer matrix method (TMM) is a very useful method especially in treating QWs with arbitrary potential profiles [17]-[19]. The method was developed to solve single-band eigensystem and later was extended to be applicable to the valence-band (heavy- and light-hole bands) of QW structures [19]. However, it was not until Chen *et al.* [30] developed a useful algorithm that the method became fully applicable to general multiband eigensystems.

We present another algorithm in the transfer matrix scheme, which is distinguished from the existing ones in algebraic steps taken for the formulation and also in its final form. On this algorithm, specific formulas are presented for the three-band [conduction band (CB), heavy-hole (HH) band, and light-hole (LH) band] and the two-band (HH and LH bands) effective-mass eigensystems. While the present method retains the advantages of the existing transfer matrix approach (it permits calculations of subband energy levels and corresponding wave functions for arbitrary shaped QW structures, where the band interactions in a given $n \times n$ multiband eigensystem are fully taken into account within the $\mathbf{k}\cdot\mathbf{p}$ approximation [31] and remote-bands effects are included by using the appropriate Luttinger parameters), the method also provides a simpler mathematical procedure and "transparent" transfer matrix characteristic in applying it to solving envelope-function equations. This is because the algebraic steps taken for the formulation are exactly the same as those in

the traditional TMMs. As a result, it maintains the conceptual simplicity and requires relatively low burden of numerical calculations.

We note that although both the present TMM and the TMM by Chen *et al.* [30] treat the multiband envelope-function equations, these two can be distinguished in the following aspects; (1) Firstly their TMM solves the equation by transforming it into a set of first-order differential equations which becomes a $2n \times 2n$ matrix equation for a given $n \times n$ effective-mass equation. The present method directly solves the $n \times n$ equation; (2) Their method needs a transformation to diagonalize the matrix exponential functions introduced in the algorithm for each spatial division along the growth direction (z-direction). The present method assumes envelope functions to take the form of $Ae^{iqz} + Be^{-iqz}$ so that it does not need this procedure; (3) Construction of envelope functions over the QW system needs to perform a retransformation process for the results obtained from a set of first order differential equations. While, in the present method, the functions are obtained by direct substitutions of the coefficients A_i and B_i into $A_i e^{iqz} + B_i e^{iqz}$.

As an illustration of the application of the method, we calculate the energy subbands of a GaAs/$Al_xGa_{1-x}As$ single QW with $x = 0.32$ and well width of 60 $\mathring{A}$. Comparisons are made between the results obtained from the three-band and two-band formulas and with the conventional variational procedure.

In the next section, we first present the formulation of the multiband TMM. Specific formulas for the two-and three-band eigensystems are also presented. In Section III sample calculations are illustrated. Finally conclusions are drawn.

II. FORMULATION OF THE METHOD

The multiband envelope function equation can be written as

$$\mathbf{H}\left(k_z \to -i\frac{\partial}{\partial z}\right)\Psi(z) = \mathbf{S}\frac{\partial^2}{\partial z^2}\Psi(z) + \mathbf{T}\frac{\partial}{\partial z}\Psi(z) + \mathbf{U}\Psi(z) = 0. \quad (1)$$

Here the multiband effective-mass Hamiltonian **H**, which forms an $n \times n$ matrix ($n = 4$ for the two-band eigensystem and n=6 for the three-band system), is divided into three parts with matrices **S**, **T**, and **U** according to order of the derivative with respect to z. The three-band and two-band effective-mass equations and corresponding matrices **S**, **T**, and **U** are discussed in Appendix.

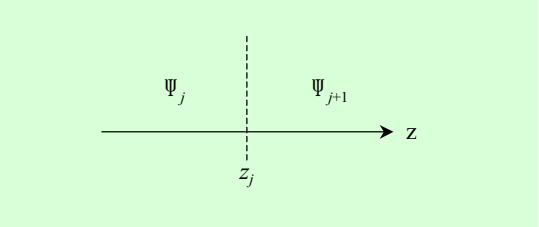

Fig. 1. Layer structure for the formulation.

As in the usual TMMs, we assume that the envelope function, solution of (1), takes the form of

$$\Psi(z) \propto e^{iqz}A + e^{-iqz}B. \tag{2}$$

For the three-band system, since particles in CB and the valence band (VB) are separated by a large energy gap, we accordingly construct their envelope functions in the j^{th} spatial division as (Fig. 1)

$$\Psi_j^{CB}(z) = \Psi_j^{CB1}(z) + \Psi_j^{CB2}(z), \tag{3}$$

$$\Psi_j^{VB}(z) = \Psi_j^{HH1}(z) + \Psi_j^{HH2}(z) + \Psi_j^{LH1}(z) + \Psi_j^{LH2}(z). \tag{4}$$

Here

$$\Psi_j^v(z) = e^{iq_j^v(z-z_{j-1})}\mathbf{V}_j^v A_j^v + e^{-iq_j^v(z-z_{j-1})}\mathbf{W}_j^v B_j^v, \tag{5}$$

where v is bulk band index (see Table 1), A and B are constant coefficients, and $\mathbf{V}_j^v$ and $\mathbf{W}_j^v$ are $n \times 1$ column vectors which are determined by

$$\mathbf{H}\left(-i\frac{\partial}{\partial z}\right)\Psi_j^V(z) = \mathbf{H}(q_j^v)e^{iq_j^v(z-z_{j-1})}\mathbf{V}_j^v A_j^v + \mathbf{H}(-q_j^v)e^{-iq_j^v(z-z_{j-1})}\mathbf{W}_j^v B_j^v = 0, \tag{6}$$

for q's evaluated from (1). This gives two eigenvalue equations

$$\mathbf{H}(q_j^v)\mathbf{V}_j^v = 0 \text{ and } \mathbf{H}(-q_j^v)\mathbf{W}_j^v = 0. \tag{7}$$

For the three-band eigensystem, these read

$$\mathbf{H}(q_j^v)\begin{bmatrix}\mathbf{V}_{j,1}^v\\ \mathbf{V}_{j,2}^v\\ \vdots\\ \mathbf{V}_{j,6}^v\end{bmatrix} = 0\begin{bmatrix}\mathbf{V}_{j,1}^v\\ \mathbf{V}_{j,2}^v\\ \vdots\\ \mathbf{V}_{j,6}^v\end{bmatrix} \quad \text{and} \quad \mathbf{H}(-q_j^v)\begin{bmatrix}\mathbf{W}_{j,1}^v\\ \mathbf{W}_{j,2}^v\\ \vdots\\ \mathbf{W}_{j,6}^v\end{bmatrix} = 0\begin{bmatrix}\mathbf{W}_{j,1}^v\\ \mathbf{W}_{j,2}^v\\ \vdots\\ \mathbf{W}_{j,6}^v\end{bmatrix}, \tag{8}$$

which represent 6×6 eigenvalue equations with zero eigenvalues and corresponding eigenvectors $\mathbf{V}_j^v$ and $\mathbf{W}_j^v$.

The coefficients A and B are determined by the boundary conditions that $\Psi(z)$ and $\mathbf{S}(\partial/\partial z)\Psi(z) + \mathbf{T}\Psi(z)$, respectively, are continuous at the interfaces. The first boundary condition, $\Psi_j(z = z_j) = \Psi_{j+1}(z = z_j)$, yields

$$\sum_v \left(\mathbf{V}_j^v A_j^v e^{iq_j^v\Delta_j} + \mathbf{W}_j^v B_j^v e^{-iq_j^v\Delta_j}\right) = \sum_v \left(\mathbf{V}_{j+1}^v A_{j+1}^v + \mathbf{W}_{j+1}^v B_{j+1}^v\right), \tag{9}$$

where v = CB1, CB2 for electrons in CB; v = HH1, HH2, LH1, LH2 for holes in VB; and $\Delta_j = z_j - z_{j-1}, \Delta_1 \equiv 0, z_0 \equiv z_1$. This can be rewritten in matrix form as

$$\mathbf{V}_j\mathbf{R}_j^{+}\mathbf{A}_j + \mathbf{W}_j\mathbf{R}_j^{-}\mathbf{B}_j = \mathbf{V}_{j+1}\mathbf{A}_{j+1} + \mathbf{W}_{j+1}\mathbf{B}_{j+1}. \tag{10}$$

Here $\mathbf{V}$ and $\mathbf{W}$ form $n \times m$ matrices, $\mathbf{R}$ an $m \times m$ matrix, and $\mathbf{A}$ and $\mathbf{B}$ $m \times 1$ matrices, where $m = 2$ for electrons in CB; i.e.,

$$\mathbf{V}_j = \begin{bmatrix} \mathbf{V}_{j,1}^{CB1} & \mathbf{V}_{j,1}^{CB2} \\ \mathbf{V}_{j,2}^{CB1} & \mathbf{V}_{j,2}^{CB2} \\ \vdots & \vdots \\ \mathbf{V}_{j,6}^{CB1} & \mathbf{V}_{j,6}^{CB2} \end{bmatrix}, \mathbf{W}_j = \begin{bmatrix} \mathbf{W}_{j,1}^{CB1} & \mathbf{W}_{j,1}^{CB2} \\ \mathbf{W}_{j,2}^{CB1} & \mathbf{W}_{j,2}^{CB2} \\ \vdots & \vdots \\ \mathbf{W}_{j,6}^{CB1} & \mathbf{W}_{j,6}^{CB2} \end{bmatrix}, \mathbf{R}_j^{\pm} = \begin{bmatrix} e^{\pm iq_j^{CB1}} & \\ & e^{\pm iq_j^{CB2}} \end{bmatrix}, \mathbf{A}_j = \begin{bmatrix} A_j^{CB1} \\ A_j^{CB2} \end{bmatrix}, \mathbf{B}_j = \begin{bmatrix} B_j^{CB1} \\ B_j^{CB2} \end{bmatrix}, \tag{11}$$

and $m = 4$ for holes in VB; i.e.,

$$\mathbf{V}_j = \begin{bmatrix} \mathbf{V}_{j,1}^{HH1} & \mathbf{V}_{j,1}^{HH2} & \mathbf{V}_{j,1}^{LH1} & \mathbf{V}_{j,1}^{LH2} \\ \mathbf{V}_{j,2}^{HH1} & \mathbf{V}_{j,2}^{HH2} & \mathbf{V}_{j,2}^{LH1} & \mathbf{V}_{j,2}^{LH2} \\ \vdots & \vdots & \vdots & \vdots \\ \mathbf{V}_{j,6}^{HH1} & \mathbf{V}_{j,6}^{HH2} & \mathbf{V}_{j,6}^{LH1} & \mathbf{V}_{j,6}^{LH2} \end{bmatrix}, \mathbf{W}_j = \begin{bmatrix} \mathbf{W}_{j,1}^{HH1} & \mathbf{W}_{j,1}^{HH2} & \mathbf{W}_{j,1}^{LH1} & \mathbf{W}_{j,1}^{LH2} \\ \mathbf{W}_{j,2}^{HH1} & \mathbf{W}_{j,2}^{HH2} & \mathbf{W}_{j,2}^{LH1} & \mathbf{W}_{j,2}^{LH2} \\ \vdots & \vdots & \vdots & \vdots \\ \mathbf{W}_{j,6}^{HH1} & \mathbf{W}_{j,6}^{HH2} & \mathbf{W}_{j,6}^{LH1} & \mathbf{W}_{j,6}^{LH2} \end{bmatrix},$$

$$\mathbf{R}_j^{\pm} = \begin{bmatrix} e^{\pm iq_j{}^{HH1}\Delta_j} & & & \\ & e^{\pm iq_j{}^{HH2}\Delta_j} & & \\ & & e^{\pm iq_j{}^{LH1}\Delta_j} & \\ & & & e^{\pm iq_j{}^{LH2}\Delta_j} \end{bmatrix}, \mathbf{A}_j = \begin{bmatrix} A_j^{HH1} \\ A_j^{HH2} \\ A_j^{LH1} \\ A_j^{LH2} \end{bmatrix}, \mathbf{B}_j = \begin{bmatrix} B_j^{HH1} \\ B_j^{HH2} \\ B_j^{LH1} \\ B_j^{LH2} \end{bmatrix} \tag{12}$$

Multiplying (10) by $\mathbf{V}_{j+1}^{-1}$ and $\mathbf{W}_{j+1}^{-1}$, respectively, from the left, we have

$$\begin{aligned} \mathbf{A}_{j+1} &= \mathbf{V}_{j+1}^{-1}\mathbf{V}_j\mathbf{R}_j^{+}\mathbf{A}_j + \mathbf{V}_{j+1}^{-1}\mathbf{W}_j\mathbf{R}_j^{-}\mathbf{B}_j - \mathbf{V}_{j+1}^{-1}\mathbf{W}_{j+1}\mathbf{B}_{j+1}, \\ \mathbf{B}_{j+1} &= \mathbf{W}_{j+1}^{-1}\mathbf{V}_j\mathbf{R}_j^{+}\mathbf{A}_j + \mathbf{W}_{j+1}^{-1}\mathbf{W}_j\mathbf{R}_j^{-}\mathbf{B}_j - \mathbf{W}_{j+1}^{-1}\mathbf{V}_{j+1}\mathbf{A}_{j+1}. \end{aligned} \tag{13}$$

Here the $m \times n$ matrices $\mathbf{V}_{j+1}^{-1}$ and $\mathbf{W}_{j+1}^{-1}$ are defined as $\mathbf{V}_{j+1}^{-1}\mathbf{V}_{j+1} = \mathbf{I}$ and $\mathbf{W}_{j+1}^{-1}\mathbf{W}_{j+1} = \mathbf{I}$, respectively, where $\mathbf{I}$ is an $m \times m$ unity matrix. It should be noted that, since $\mathbf{W}$ and $\mathbf{V}$ are not square matrices, the order of multiplication in the above definition should be respected.

The second boundary condition of

$$\mathbf{S}_j\frac{\partial}{\partial z}\Psi_j(z = z_j) + \mathbf{T}_j\Psi_j(z = z_j) = \mathbf{S}_{j+1}\frac{\partial}{\partial z}\Psi_{j+1}(z = z_j) + \mathbf{T}_{j+1}\Psi_{j+1}(z = z_j) \tag{14}$$

yields

$$\sum_v \left(\mathbf{S}_j\mathbf{V}_j^v iq_j^v A_j^v e^{iq_j{}^v\Delta_j} - \mathbf{S}_j\mathbf{W}_j^v iq_j^v B_j^v e^{-iq_j^v\Delta_j} + \mathbf{T}_j\mathbf{V}_j^v A_j^v e^{iq_j^v\Delta_j} + \mathbf{T}_j\mathbf{W}_j^v B_j^v e^{-iq_j^v\Delta_j}\right)$$
$$= \sum_v \left(\mathbf{S}_{j+1}\mathbf{V}_{j+1}^v iq_{j+1}^v A_{j+1}^v - \mathbf{S}_{j+1}\mathbf{W}_{j+1}^v iq_{j+1}^v B_{j+1}^v + \mathbf{T}_{j+1}\mathbf{V}_{j+1}^v A_{j+1}^v + \mathbf{T}_{j+1}\mathbf{W}_{j+1}^v B_{j+1}^v\right). \quad (15)$$

This can also be rewritten in matrix form as

$$\mathbf{S}_j\mathbf{V}_j\mathbf{Q}_j\mathbf{R}_j^+\mathbf{A}_j - \mathbf{S}_j\mathbf{W}_j\mathbf{Q}_j\mathbf{R}_j^-\mathbf{B}_j + \mathbf{T}_j\mathbf{V}_j\mathbf{R}_j^+\mathbf{A}_j + \mathbf{T}_j\mathbf{W}_j\mathbf{R}_j^-\mathbf{B}_j$$
$$= \mathbf{S}_{j+1}\mathbf{V}_{j+1}\mathbf{Q}_{j+1}\mathbf{A}_{j+1} - \mathbf{S}_{j+1}\mathbf{W}_{j+1}\mathbf{Q}_{j+1}\mathbf{B}_{j+1} + \mathbf{T}_{j+1}\mathbf{V}_{j+1}\mathbf{A}_{j+1} + \mathbf{T}_{j+1}\mathbf{W}_{j+1}\mathbf{B}_{j+1}, \quad (16)$$

where $\mathbf{Q}$ is an $m \times m$ matrix:

$$Q_j = \begin{bmatrix} iq_j^{CB1} & \\ & iq_j^{CB2} \end{bmatrix} \quad \text{and} \quad Q_j = \begin{bmatrix} iq_j^{HH1} & & & \\ & iq_j^{HH2} & & \\ & & iq_j^{LH1} & \\ & & & iq_j^{LH2} \end{bmatrix}. \quad (17)$$

for CB and VB, respectively.

Substituting (13) into (16), we finally obtain equations for A and B:

$$\left[\mathbf{S}_{j+1}\mathbf{V}_{j+1}\mathbf{Q}_{j+1} + \mathbf{S}_{j+1}\mathbf{W}_{j+1}\mathbf{Q}_{j+1}\mathbf{W}_{j+1}^{-1}\mathbf{V}_{j+1}\right]\mathbf{A}_{j+1}$$
$$= \left[\mathbf{S}_{j+1}\mathbf{W}_{j+1}\mathbf{Q}_{j+1}\mathbf{W}_{j+1}^{-1}\mathbf{V}_j\mathbf{R}_j^+ + \mathbf{S}_j\mathbf{V}_j\mathbf{Q}_j\mathbf{R}_j^+ - \mathbf{T}_{j+1}\mathbf{V}_j\mathbf{R}_j^+ + \mathbf{T}_j\mathbf{V}_j\mathbf{R}_j^+\right]\mathbf{A}_j$$
$$+ \left[\mathbf{S}_{j+1}\mathbf{W}_{j+1}\mathbf{Q}_{j+1}\mathbf{W}_{j+1}^{-1}\mathbf{W}_j\mathbf{R}_j^- - \mathbf{S}_j\mathbf{W}_j\mathbf{Q}_j\mathbf{R}_j^- - \mathbf{T}_{j+1}\mathbf{W}_j\mathbf{R}_j^- + \mathbf{T}_j\mathbf{W}_j\mathbf{R}_j^-\right]\mathbf{B}_j, \quad (18)$$
$$\left[\mathbf{S}_{j+1}\mathbf{W}_{j+1}\mathbf{Q}_{j+1} + \mathbf{S}_{j+1}\mathbf{V}_{j+1}\mathbf{Q}_{j+1}\mathbf{V}_{j+1}^{-1}\mathbf{W}_{j+1}\right]\mathbf{B}_{j+1}$$
$$= \left[\mathbf{S}_{j+1}\mathbf{V}_{j+1}\mathbf{Q}_{j+1}\mathbf{V}_{j+1}^{-1}\mathbf{V}_j\mathbf{R}_j^+ - \mathbf{S}_j\mathbf{V}_j\mathbf{Q}_j\mathbf{R}_j^+ + \mathbf{T}_{j+1}\mathbf{V}_j\mathbf{R}_j^+ - \mathbf{T}_j\mathbf{V}_j\mathbf{R}_j^+\right]\mathbf{A}_j$$
$$+ \left[\mathbf{S}_{j+1}\mathbf{V}_{j+1}\mathbf{Q}_{j+1}\mathbf{V}_{j+1}^{-1}\mathbf{W}_j\mathbf{R}_j^- + \mathbf{S}_j\mathbf{W}_j\mathbf{Q}_j\mathbf{R}_j^- + \mathbf{T}_{j+1}\mathbf{W}_j\mathbf{R}_j^- - \mathbf{T}_j\mathbf{W}_j\mathbf{R}_j^-\right]\mathbf{B}_j, \quad (19)$$

These can be combined in matrix form as

$$\begin{bmatrix} \mathbf{A}_{j+1} \\ \mathbf{B}_{j+1} \end{bmatrix} = \begin{bmatrix} \mathbf{M}_{11} & \mathbf{M}_{12} \\ \mathbf{M}_{21} & \mathbf{M}_{22} \end{bmatrix} \begin{bmatrix} \mathbf{A}_j \\ \mathbf{B}_j \end{bmatrix} = \mathbf{M}_j \begin{bmatrix} \mathbf{A}_j \\ \mathbf{B}_j \end{bmatrix}, \quad (20)$$

where $\mathbf{M}_{ab}(a,b=1,2)$ forms an $m \times m$ matrix, and the multiband transfer matrix is defined as

$$\mathbf{M}_j = \begin{bmatrix} \mathbf{S}_{j+1}\mathbf{W}_{j+1}\mathbf{Q}_{j+1}\mathbf{W}_{j+1}^{-1}\mathbf{V}_{j+1} + \mathbf{S}_{j+1}\mathbf{V}_{j+1}\mathbf{Q}_{j+1} & \\ & \mathbf{S}_{j+1}\mathbf{V}_{j+1}\mathbf{Q}_{j+1}\mathbf{V}_{j+1}^{-1}\mathbf{W}_{j+1} + \mathbf{S}_{j+1}\mathbf{W}_{j+1}\mathbf{Q}_{j+1} \end{bmatrix}^{-1}$$

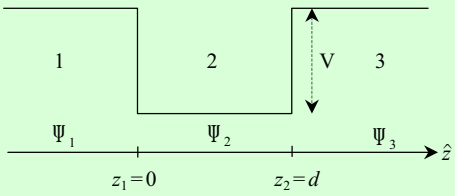

Fig. 2. Single quantum well structure.

$$\times \begin{bmatrix} \mathbf{S}_{j+1}\mathbf{W}_{j+1}\mathbf{Q}_{j+1}\mathbf{W}_{j+1}^{-1}\mathbf{V}_j + \mathbf{S}_j\mathbf{V}_j\mathbf{Q}_j - \mathbf{T}_{j+1}\mathbf{V}_j + \mathbf{T}_j\mathbf{V}_j & \mathbf{S}_{j+1}\mathbf{W}_{j+1}\mathbf{Q}_{j+1}\mathbf{W}_{j+1}^{-1}\mathbf{W}_j - \mathbf{S}_j\mathbf{W}_j\mathbf{Q}_j - \mathbf{T}_{j+1}\mathbf{W}_j + \mathbf{T}_j\mathbf{W}_j \\ \mathbf{S}_{j+1}\mathbf{V}_{j+1}\mathbf{Q}_{j+1}\mathbf{V}_{j+1}^{-1}\mathbf{V}_j - \mathbf{S}_j\mathbf{V}_j\mathbf{Q}_j + \mathbf{T}_{j+1}\mathbf{V}_j - \mathbf{T}_j\mathbf{V}_j & \mathbf{S}_{j+1}\mathbf{V}_{j+1}\mathbf{Q}_{j+1}\mathbf{V}_{j+1}^{-1}\mathbf{W}_j + \mathbf{S}_j\mathbf{W}_j\mathbf{Q}_j + \mathbf{T}_{j+1}\mathbf{W}_j - \mathbf{T}_j\mathbf{W}_j \end{bmatrix}$$

$$\times \begin{bmatrix} \mathbf{R}_j^+ & \\ & \mathbf{R}_j^- \end{bmatrix}. \tag{21}$$

1. Quantum Well Structures

For a QW structure with arbitrary potential profile, the present method can be applied by dividing the potential into several layers with constant potential profiles. By repeatedly applying (20) to an r-layer structure, we can find a relation between A and B coefficients in the outermost layers:

$$\begin{bmatrix} \mathbf{A}_r \\ \mathbf{B}_r \end{bmatrix} \mathbf{M}_{r-1}\cdots\mathbf{M}_2\mathbf{M}_1 \begin{bmatrix} \mathbf{A}_1 \\ \mathbf{B}_2 \end{bmatrix} \equiv \begin{bmatrix} \Lambda_{11} & \Lambda_{12} \\ \Lambda_{21} & \Lambda_{22} \end{bmatrix} \begin{bmatrix} \mathbf{A}_1 \\ \mathbf{B}_2 \end{bmatrix}. \tag{22}$$

The envelope functions should be bound in space so that they should be zero in amplitude when z tends to plus or minus infinity. This boundary condition requires that

$$\mathbf{A}_1 = \begin{bmatrix} 0 \\ \vdots \\ 0 \end{bmatrix} \quad \text{and} \quad \mathbf{B}_r = \begin{bmatrix} 0 \\ \vdots \\ 0 \end{bmatrix}, \tag{23}$$

which dictates

$$\text{Det } \Lambda_{22} = 0. \tag{24}$$

Eigenvalues $\mathcal{E}$ are determined by this requirement.

To help understanding of the proposed method, a simple application of the two-band formula is made to a single QW (Fig. 2). As the purpose of this example is to show how the method is applied to the multi-band eigensystem on the same line of the single-band TMM, we assume $k_x = k_y = 0$ and ignore the band-parameter difference to make the problem simplest. We note that the original dimension of the two-band eigensystem, $n = 4$, can be reduced to $n = 2$ in this case.

The matrices included in the formula are given as

$$\mathbf{S}_j = \frac{\hbar^2}{2m_0}\begin{bmatrix}(\gamma_1 - 2\gamma_2)_j & \\ & (\gamma_1 + 2\gamma_2)_j\end{bmatrix}, \quad \mathbf{T}_j = [0], \mathbf{V}_j = \mathbf{W}_j = \mathbf{I}, \; \mathbf{R}_1^+ = \mathbf{R}_1^- = \mathbf{I},$$

$$\mathbf{R}_2^{\pm} = \begin{bmatrix}e^{\pm i\beta_h} & \\ & e^{\pm i\beta_l}\end{bmatrix}, \; \mathbf{R}_3^{\pm} = \begin{bmatrix}e^{\mp\alpha_h} & \\ & e^{\mp\alpha_l}\end{bmatrix}, \; \mathbf{Q}_1 = \mathbf{Q}_3 = \begin{bmatrix}-\alpha_h & \\ & -\alpha_l\end{bmatrix}, \; \mathbf{Q}_2 = \begin{bmatrix}i\beta_h & \\ & i\beta_l\end{bmatrix}, \tag{25}$$

where $[0]$ is an 2×2 null matrix, $\mathbf{I}$ 2×2 unity matrix, and

$$\alpha_{h,l} = \left(\frac{2m}{\hbar^2(\gamma_1 \mp 2\gamma_2)}\right)^{1/2}\sqrt{\mathcal{E} - V}, \; \beta_{h,l} = \left(\frac{2m}{\hbar^2(\gamma_1 \mp 2\gamma_2)}\right)^{1/2}\sqrt{\mathcal{E}}. \tag{26}$$

Envelope function coefficients are calculated by substituting (25) into (20):

$$\begin{bmatrix}A_2^h \\ A_2^l \\ B_2^h \\ B_2^l\end{bmatrix} = \frac{1}{2}\begin{bmatrix}\begin{bmatrix}1/i\beta_h & \\ & 1/i\beta_l\end{bmatrix} & \\ & \begin{bmatrix}1/i\beta_h & \\ & 1/i\beta_l\end{bmatrix}\end{bmatrix}\begin{bmatrix}\begin{bmatrix}i\beta_h - \alpha_h & \\ & i\beta_l - \alpha_l\end{bmatrix} & \begin{bmatrix}i\beta_h + \alpha_h & \\ & i\beta_l + \alpha_l\end{bmatrix} \\ \begin{bmatrix}i\beta_h + \alpha_h & \\ & i\beta_l + \alpha_l\end{bmatrix} & \begin{bmatrix}i\beta_h - \alpha_h & \\ & i\beta_l - \alpha_l\end{bmatrix}\end{bmatrix}\begin{bmatrix}\begin{bmatrix}1 & \\ & 1\end{bmatrix} & \\ & \begin{bmatrix}1 & \\ & 1\end{bmatrix}\end{bmatrix}\begin{bmatrix}A_1^h \\ A_1^l \\ B_1^h \\ B_1^l\end{bmatrix}, \tag{27}$$

$$\begin{bmatrix}A_3^h \\ A_3^l \\ B_3^h \\ B_3^l\end{bmatrix} = -\frac{1}{2}\begin{bmatrix}\begin{bmatrix}1/\alpha_h & \\ & 1/\alpha_l\end{bmatrix} & \\ & \begin{bmatrix}1/\alpha_h & \\ & 1/\alpha_l\end{bmatrix}\end{bmatrix}\begin{bmatrix}\begin{bmatrix}-\alpha_h + i\beta_h & \\ & -\alpha_h + i\beta_l\end{bmatrix} & \begin{bmatrix}-\alpha_h - i\beta_h & \\ & -\alpha_l - i\beta_l\end{bmatrix} \\ \begin{bmatrix}-\alpha_h - i\beta_h & \\ & -\alpha_l - i\beta_l\end{bmatrix} & \begin{bmatrix}-\alpha_h + i\beta_h & \\ & -\alpha_l + i\beta_l\end{bmatrix}\end{bmatrix}\begin{bmatrix}\begin{bmatrix}e^{i\beta_h d} & \\ & e^{i\beta_l d}\end{bmatrix} & \\ & \begin{bmatrix}e^{-i\beta_h d} & \\ & e^{-i\beta_l d}\end{bmatrix}\end{bmatrix}\begin{bmatrix}A_2^h \\ A_2^l \\ B_2^h \\ B_2^l\end{bmatrix} \tag{28}$$

Corresponding equation to (24) is

$$\Lambda_{22} = \begin{bmatrix}\dfrac{2i(\alpha_h^2 - \beta_h^2)\sin(\beta_h d) + 4i\alpha_h\beta_h\cos(\beta_h d)}{4i\alpha_h\beta_h} & \\ & \dfrac{2i(\alpha_l^2 - \beta_l^2)\sin(\beta_l d) + 4i\alpha_l\beta_l\cos(\beta_l d)}{4i\alpha_l\beta_l}\end{bmatrix}. \tag{29}$$

Eigenvalues are obtained by $|\Lambda_{22}| = 0$, which gives the usual equations for the simple QW [32]:

$$\frac{\alpha_v^2 - \beta_v^2}{2\alpha_v\beta_v} = -\frac{\cos(\beta_v d)}{\sin(\beta_v d)}, \tag{30}$$

with v= h,l. Corresponding envelope functions are immediately obtained as

$$\begin{bmatrix}\Psi_1^h\\ \Psi_1^l\end{bmatrix}=\begin{bmatrix}e^{\alpha_h z}\\ e^{\alpha_l z}\end{bmatrix}B_1,\quad \begin{bmatrix}\Psi_2^h\\ \Psi_2^l\end{bmatrix}=\begin{bmatrix}\cos(\beta_h z)+\dfrac{\alpha_h}{\beta_h}\sin(\beta_h z)\\ \cos(\beta_l z)+\dfrac{\alpha_l}{\beta_l}\sin(\beta_l z)\end{bmatrix}B_1,\quad \begin{bmatrix}\Psi_3^h\\ \Psi_3^l\end{bmatrix}=\begin{bmatrix}e^{-\alpha_h z}\\ e^{-\alpha_l z}\end{bmatrix}B_1. \tag{31}$$

The constant B_1 is determined by the normalization of the envelope functions.

2. Superlattice Structures

The extension of the method to SL is straightforward. For the SL structure with period d, energies and corresponding envelope functions can be determined using the Bloch condition for the SL:

$$\Psi_{p+2}(z_{p+2})=e^{iq_s d}\Psi_p(z_p), \tag{32}$$

which leads to

$$\begin{bmatrix}\mathbf{A}_{p+2}\\ \mathbf{B}_{p+2}\end{bmatrix}=e^{iq_s d}\begin{bmatrix}\mathbf{A}_p\\ \mathbf{B}_p\end{bmatrix}, \tag{33}$$

where q_s is the SL wave vector. If we set

$$\begin{bmatrix}\mathbf{A}_{p+2}\\ \mathbf{B}_{p+2}\end{bmatrix}=\begin{bmatrix}\mathbf{M}_{p+1}^{11}\,\mathbf{M}_{p+1}^{12}\\ \mathbf{M}_{p+1}^{21}\,\mathbf{M}_{p+1}^{22}\end{bmatrix}\begin{bmatrix}\mathbf{M}_p^{11}\,\mathbf{M}_p^{12}\\ \mathbf{M}_p^{21}\,\mathbf{M}_p^{22}\end{bmatrix}\equiv\begin{bmatrix}\mathbf{P}_{11}\,\mathbf{P}_{12}\\ \mathbf{P}_{21}\,\mathbf{P}_{22}\end{bmatrix}\begin{bmatrix}\mathbf{A}_p\\ \mathbf{B}_p\end{bmatrix}, \tag{34}$$

then we obtain

$$\begin{bmatrix}\mathbf{P}_{11}\,\mathbf{P}_{12}\\ \mathbf{P}_{21}\,\mathbf{P}_{22}\end{bmatrix}\begin{bmatrix}\mathbf{A}_p\\ \mathbf{B}_p\end{bmatrix}=e^{iq_s d}\begin{bmatrix}\mathbf{A}_p\\ \mathbf{B}_p\end{bmatrix}\quad\text{or}\quad\begin{bmatrix}\mathbf{P}_{11}-\mathbf{I}e^{iq_x d} & \mathbf{P}_{12}\\ \mathbf{P}_{21} & \mathbf{P}_{22}-\mathbf{I}e^{iq_s d}\end{bmatrix}\begin{bmatrix}\mathbf{A}_p\\ \mathbf{B}_P\end{bmatrix}=\begin{bmatrix}[0]\\ [0]\end{bmatrix}, \tag{35}$$

where [0] represents an $m\times 1$ null column vector. Thus eigenvalues can be determined by vanishing determinant of the coefficient matrix of (35):

$$\mathrm{Det}\begin{bmatrix}\mathbf{P}_{11}-\mathbf{I}e^{iq_s d} & \mathbf{P}_{12}\\ \mathbf{P}_{21} & \mathbf{P}_{22}-\mathbf{I}e^{iq_s d}\end{bmatrix}=0. \tag{36}$$

We also make an application of the two-band formula to a simple SL (Fig. 3) for the same

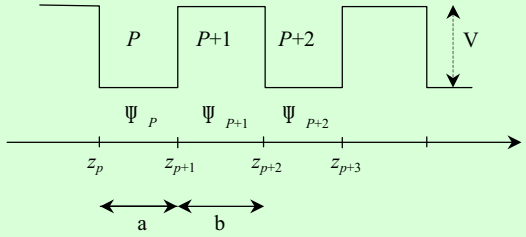

Fig. 3. Superlattice structure.

purpose as in the previous subsection. We again assume $k_x = k_y = 0$ and ignore the band-parameter difference. The original dimension of the two-band eigensystem is reduced to $n = 2$ in this case too.

Envelope function coefficients in $(k+1)^{\text{th}}$ and $(k+2)^{\text{th}}$ layers are calculated, respectively, by substituting (25) into (20):

$$\begin{bmatrix} A^h_{k+1} \\ A^l_{k+1} \\ B^h_{k+1} \\ B^l_{k+1} \end{bmatrix} = \frac{1}{2} \begin{bmatrix} 1/i\beta_h & & & \\ & 1/i\beta_l & & \\ & & 1/i\beta_h & \\ & & & 1/i\beta_l \end{bmatrix} \begin{bmatrix} i\beta_h - \alpha_h & & i\beta_h + \alpha_h & \\ & i\beta_l - \alpha_l & & i\beta_l + \alpha_l \\ i\beta_h + \alpha_h & & i\beta_h - \alpha_h & \\ & i\beta_l + \alpha_l & & i\beta_l - \alpha_l \end{bmatrix} \begin{bmatrix} e^{-i\alpha_h a} & & & \\ & e^{-i\alpha_l a} & & \\ & & e^{\alpha_h a} & \\ & & & e^{\alpha_l a} \end{bmatrix} \begin{bmatrix} A^h_k \\ A^l_k \\ B^h_k \\ B^l_k \end{bmatrix}$$

$$= \frac{1}{2} \begin{bmatrix} 1/i\beta_h & & & \\ & 1/i\beta_l & & \\ & & 1/i\beta_h & \\ & & & 1/i\beta_l \end{bmatrix} \begin{bmatrix} (i\beta_h - \alpha_h)e^{-\alpha_h a} & & (i\beta_h + \alpha_h)e^{\alpha_h a} & \\ & (i\beta_l - \alpha_l)e^{-\alpha_l a} & & (i\beta_h + \alpha_l)e^{\alpha_l a} \\ (i\beta_h + \alpha_h)e^{-\alpha_h a} & & (i\beta_h - \alpha_h)e^{\alpha_h a} & \\ & (i\beta_l + \alpha_l)e^{-\alpha_l a} & & (i\beta_l - \alpha_l)e^{\alpha_l a} \end{bmatrix} \begin{bmatrix} A^h_k \\ A^l_k \\ B^h_k \\ B^l_k \end{bmatrix}, \tag{37}$$

$$\begin{bmatrix} A^h_{k+2} \\ A^l_{k+2} \\ B^h_{k+2} \\ B^l_{k+2} \end{bmatrix} = \frac{1}{2} \begin{bmatrix} 1/\alpha_h & & & \\ & 1/\alpha_l & & \\ & & 1/\alpha_h & \\ & & & 1/\alpha_l \end{bmatrix} \begin{bmatrix} (\alpha_h - i\beta_h)e^{i\beta_h b} & & (\alpha_h + i\beta_h)e^{-i\beta_h b} & \\ & (\alpha_l - i\beta_l)e^{i\beta_l b} & & (\alpha_l + i\beta_l)e^{-i\beta_l b} \\ (\alpha_h + i\beta_h)e^{i\beta_h b} & & (\alpha_h - i\beta_h)e^{-i\beta_h b} & \\ & (\alpha_l + i\beta_l)e^{i\beta_l b} & & (\alpha_l - i\beta_l)e^{-i\beta_l b} \end{bmatrix} \begin{bmatrix} A^h_{k+1} \\ A^l_{k+1} \\ B^h_{k+1} \\ B^l_{k+1} \end{bmatrix}$$

$$= \begin{bmatrix} \frac{1}{4i\alpha_h\beta_h} & & & \\ & \frac{1}{4i\alpha_l\beta_l} & & \\ & & \frac{1}{4i\alpha_h\beta_h} & \\ & & & \frac{1}{4i\alpha_l\beta_l} \end{bmatrix} \begin{bmatrix} \frac{1}{2}i(\beta_h^2 - \alpha_h^2)e^{-\alpha_h a}\sin\beta b & & \frac{1}{2}i(\beta_h^2 + \alpha_h^2)e^{\alpha_h a}\sin\beta b & \\ +i\alpha_h\beta_h e^{-\alpha_h a}\cos\beta b & & & \\ & \frac{1}{2}i(\beta_l^2 - \alpha_l^2)e^{-\alpha_l a}\sin\beta b & & \frac{1}{2}i(\beta_l^2 + \alpha_l^2)e^{\alpha_l a}\sin\beta b \\ & +i\alpha_l\beta_l e^{-\alpha_h a}\cos\beta b & & \\ -\frac{1}{2}i(\beta_h^2 + \alpha_h^2)e^{-\alpha_h a}\sin\beta b & & \frac{1}{2}i(\alpha_h^2 - \beta_h^2)e^{\alpha_h a}\sin\beta b & \\ & -\frac{1}{2}i(\beta_l^2 + \alpha_l^2)e^{-\alpha_l a}\sin\beta b & +i\alpha_h\beta_h e^{\alpha_h a}\cos\beta b & \\ & & & \frac{1}{2}i(\alpha_l^2 - \beta_l^2)e^{\alpha_l a}\sin\beta b \\ & & & +i\alpha_l\beta_l e^{\alpha_h a}\cos\beta b \end{bmatrix} \begin{bmatrix} A^h_k \\ A^l_k \\ B^h_k \\ B^l_k \end{bmatrix}, \tag{38}$$

Comparing (38) with (36), we obtain

$$\mathrm{Det}\begin{bmatrix} \begin{bmatrix} \frac{1}{2}i(\beta_h^2-\alpha_h^2)e^{-\alpha_h a}\sin\beta b \\ +i\alpha_h\beta_h e^{-\alpha_h a}\cos\beta b \end{bmatrix} & \begin{bmatrix} \frac{1}{2}i(\beta_h^2+\alpha_h^2)e^{\alpha_h a}\sin\beta b \\ \frac{1}{2}i(\beta_l^2+\alpha_l^2)e^{\alpha_l a}\sin\beta b \end{bmatrix} \\ \begin{bmatrix} -\frac{1}{2}i(\beta_h^2+\alpha_h^2)e^{-\alpha_h a}\sin\beta b \\ -\frac{1}{2}i(\beta_l^2+\alpha_l^2)e^{-\alpha_l a}\sin\beta b \end{bmatrix} & \begin{bmatrix} \frac{1}{2}i(\alpha_h^2-\beta_h^2)e^{\alpha_h a}\sin\beta b \\ +i\alpha_h\beta_h e^{\alpha_h a}\cos\beta b \\ \frac{1}{2}i(\alpha_l^2-\beta_l^2)e^{\alpha_l a}\sin\beta b \\ +i\alpha_h\beta_h e^{\alpha_h a}\cos\beta b \end{bmatrix} \end{bmatrix} = 0, \tag{39}$$

which gives the usual Kronig-Penney solutions: [32]

$$\frac{\alpha_v^2-\beta_v^2}{2\alpha_v\beta_v}\sin\beta_v b\sinh\alpha_v a+\cos\beta_v b\cosh\alpha_v a=\cos qd, \tag{40}$$

where $v=h,l$.

III. SAMPLE CALCULATIONS FOR A GaAs/AlGaAs SINGLE QUANTUM WELL

In this section we attempt numerical computations to compare the results obtained based on various multiband effective-mass eigensystems and to show validity of the method. In the calculations caution needs to be taken for spurious solutions which can occur in finding zeros of the determinant. These solutions arise when the bulk wave functions are not linearly independent in the cases that the wave vector along the z-direction, q, vanishes or $q^H=q^L$ for the two-band eigensystem [26].

We take a GaAs/AlGaAs single QW with an aluminum mole fraction $x=0.32$ in the barriers and a well width of 60 $\mathring{\mathrm{A}}$ (Fig. 4). The band interaction parameters, including the Luttinger parameters, in the effective-mass Hamiltonian formalism depend on the number of basis bands included in the Hamiltonian as well as the type of material. Values of band parameters for the given Al mole fraction were obtained by linear interpolation between the values for GaAs and AlAs. The band gap difference in eV is taken to be $\Delta\mathcal{E}=1.247x$ [33]. We assume a 40/60 % split for the discontinuities of the valence and conduction bands [34], which gives values of potential barriers $V_c=240$ meV in CB and $V_v=160$ meV in VB. The zero of the energy was taken to coincide with the top of the bulk GaAs valence band. The evaluation of pertinent parameters are presented in Appendix. In the calculations we neglect all inversion asymmetry in the III-V compound, which leads to a Kramer's degeneracy for the bands.

Figure 5 compares the VB subband energy structures of the model QW obtained using the two-band formula and using the variational method [34]. The difference in the band parameters between the two adjacent layers is ignored to obtain a proper

comparison, as the difference was neglected in the variational calculation. As seen from the figure, the two results are in close agreement. The figure also indicates that the band-parameter difference does not produce considerable effects on the subband energies for this type of QW system due to similarity in band parameters between the two materials, as previously pointed out many times [2].

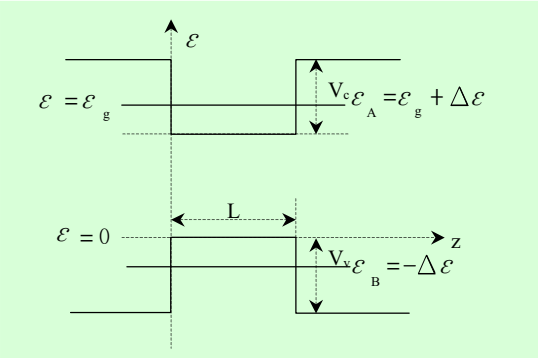

Fig. 4. Band structure of the three-band quantum well eigensystem.

We compare the CB subband energy structure obtained by the three-band formula with that obtained by the single-band TMM. As seen from Fig. 6, confined energies in CB obtained by the three-band formula show the typical nonparabolic characteristic as in the case of bulk material [35], [36]. The conduction band nonparabolicity has an important influence on the intersubband absorption line broadening [37] and cannot be obtained by any method based on the single-band effective-mass equation.

Figure 7 shows that the LH subband energies by the three-band formula disagree

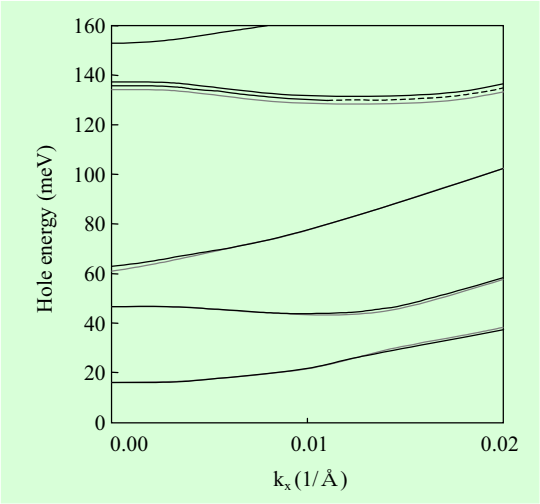

Fig. 5. Valence band subband energies. From the bottom, the subbands are HH1, LH1, HH2, HH3, and LH2. The solid lines were obtained by the variational method; and the dotted by the two-band transfer matrix formula, where the band-parameter differences between layers were ignored as in solid lines. The dashed lines were obtained by the two-band formula, where the band-parameter differences were taken into account.

by about 10 meV at maximum with those obtained by the two-band formula. This is because the LH band, as compared with the HH band, is strongly coupled to CB so that a stronger modification occurs in LH subbands when the interaction between CB and VB are included. As seen from the figure, the effect of the band-parameter difference on the valence subband energies is insignificant except on the LH1 subband energies; however the effect on the conduction subband energies is somewhat larger, which causes 5–10 meV difference in energy (Fig. 6).

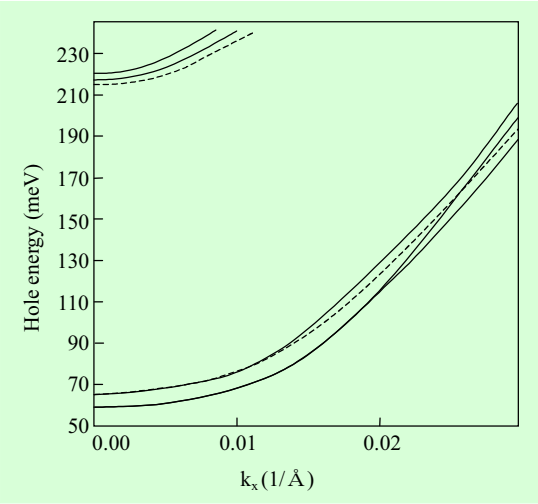

Fig. 6. Conduction band subband energies. The solid and dotted lines were obtained by the three-band formula and dashed and dash-dotted lines by the single-band transfer matrix formula. The band-parameter differences were taken into account in solid and dashed lines, while not in the dotted and dash-dotted lines.

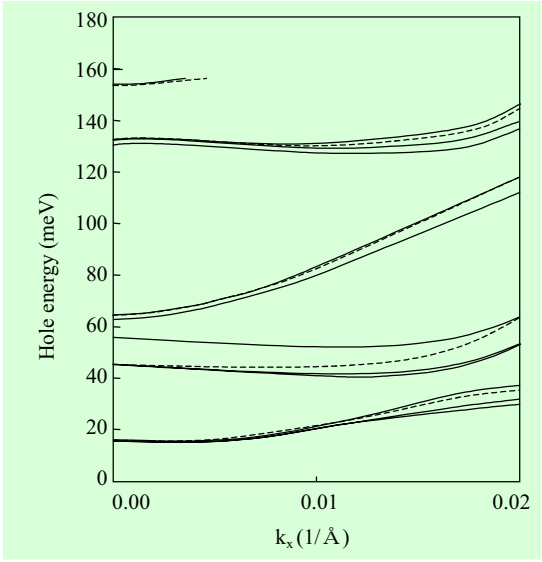

Fig. 7. Valence band subband energies. Solid and dotted lines were obtained by the three-band formula and the dashed and dash-dotted lines by the two-band formula. The band-parameter differences were taken into account in solid and dashed lines, while not in the dotted and dash-dotted lines.

IV. CONCLUSIONS

We presented an improved transfer matrix method developed by taking different algebraic steps from the existing methods. The present method retains the advantages in the existing approach including the capability of calculating subband energies and corresponding wave functions for arbitrary shaped QW structures, where the band interactions in an $n \times n$ multiband eigensystem are fully taken into account within the $\mathbf{k}\cdot\mathbf{p}$ approximation. The method also provides a simpler mathematical procedure and "transparent" transfer matrix characteristic in its application to the problem, as algebraic steps taken for the formulation are exactly the same as those of the traditional TMMs. As a result, it retains the conceptual simplicity of the usual TMM and lays less burden of numerical calculations.

As an illustration of the application of the method, numerical computations were made for a single GaAs/AlGaAs QW by both the two-band and three-band formulae and compared the results with those obtained by the conventional variational procedure to assess the validity of the method. The $\mathcal{E}-\mathbf{k}_t$ (energy-inplane wave vector) dispersions calculated with the two-band

formula are in close agreement with those from the variational procedure. The results with the three-band formula are in general agreement with those obtained by the single- (for the conduction band) and the two-band (for the heavy- and light-hole bands) TMM formulas; however the confined energies in the conduction band calculated by the three-band formula show the expected nonparabolic characteristic. The three-band formula revealed the strong coupling between CB and LH band by showing that the conduction and LH subband energies changed by about 10 meV at maximum from those obtained with the two-band formula.

ACKNOWLEDGMENTS

One of the authors (B.W. Kim) thanks Prof. A. Majerfeld for a critical review of the manuscript. The authors wish to acknowledge Dr. K.C. Park, Mr. S.R. Kang, and Dr. C.H. Yim in ETRI for supporting this work.

APPENDIX

A three-band effective-mass Hamiltonian is constructed by replacing k_z in the bulk Hamiltonian by $-i\partial/\partial z$ and is given in Table 1. [38]

The quantities included in Table 1 are defined as

$$F = \mathcal{E}_v - \frac{\hbar^2}{2m_0}\left[(\gamma_1+\gamma_2)(k_x^2+k_y^2)+(\gamma_1-2\gamma_2)\frac{\partial^2}{\partial z^2}\right] + V_v - \mathcal{E},$$

$$G = \mathcal{E}_v - \frac{\hbar^2}{2m_0}\left[(\gamma_1-\gamma_2)(k_x^2+k_y^2)+(\gamma_1+2\gamma_2)\frac{\partial^2}{\partial z^2}\right] + V_v - \mathcal{E},$$

$$M = -i\frac{\hbar^2}{2m_0}2\sqrt{3}\gamma_3(k_x+ik_y)\frac{\partial}{\partial z},$$

$$N = \frac{\hbar^2}{2m_0}\left[\sqrt{3}\gamma_2(k_y^2-k_x^2)+i2\sqrt{3}\gamma_3 k_x k_y\right],$$

$$\pi = \frac{\hbar}{m_0}\left\langle S\right|-i\hbar\frac{\partial}{\partial x}\left|X\right\rangle. \quad \text{(A1)}$$

The basis functions for this equation are

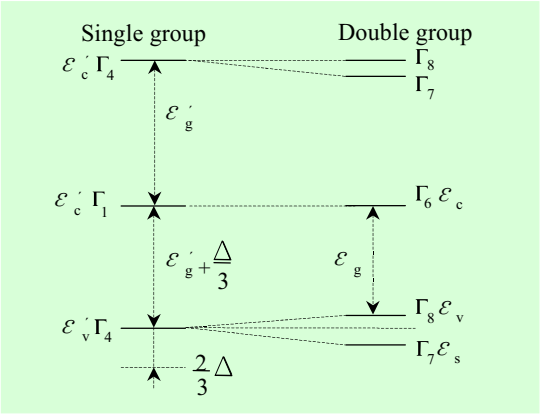

Fig. 8. Energy level structure of showing the single and double groups for zinc-blende lattice.

chosen as

$$\mathrm{CB1}(\Gamma_6,1/2) = |s\rangle\uparrow,$$

$$\mathrm{CB2}(\Gamma_6,-1/2) = |s\rangle\downarrow,$$

$$\mathrm{HH1}(\Gamma_8,3/2) = \frac{1}{\sqrt{2}}|(X+iY)\rangle\uparrow,$$

$$\mathrm{HH2}(\Gamma_8,-3/2) = \frac{1}{\sqrt{2}}|(iX+Y)\rangle\downarrow,$$

$$\mathrm{LH1}(\Gamma_8,1/2) = \frac{1}{\sqrt{6}}|(iX-Y)\rangle\downarrow -i\frac{\sqrt{2}}{\sqrt{3}}|Z\rangle\uparrow,$$

$$\mathrm{LH2}(\Gamma_8,-1/2) = \frac{1}{\sqrt{6}}|(X-iY)\rangle\uparrow+\frac{\sqrt{2}}{\sqrt{3}}|Z\rangle\downarrow, \quad \text{(A2)}$$

Table 1. Three-band effective-mass Hamiltonian.

	CB1	CB2	HH1	HH2	LH1	LH2
CB1	$\mathcal{E}_c+\frac{\hbar^2k^2}{2m_0'}+V_c-\mathcal{E}$	0	$\frac{1}{\sqrt{2}}\pi(k_x+ik_y)$	0	$-\sqrt{\frac{2}{3}}\pi\frac{\partial}{\partial z}$	$\frac{1}{\sqrt{6}}\pi(k_x-ik_y)$
CB2	0	$\mathcal{E}_c+\frac{\hbar^2k^2}{2m_0'}+V_c-\mathcal{E}$	0	$\frac{i}{\sqrt{2}}\pi(k_x-ik_y)$	$\frac{i}{\sqrt{6}}\pi(k_x+ik_y)$	$-i\sqrt{\frac{2}{3}}\pi\frac{\partial}{\partial z}$
HH1	$\frac{1}{\sqrt{2}}\pi(k_x-ik_y)$	0	F	0	M	N
HH2	0	$\frac{-i}{\sqrt{2}}\pi(k_x+ik_y)$	0	F	N^*	$-M$
LH1	$\sqrt{\frac{2}{3}}\pi\frac{\partial}{\partial z}$	$\frac{-i}{\sqrt{6}}\pi(k_x-ik_y)$	M	N	G	0
LH2	$\frac{1}{\sqrt{6}}\pi(k_x+ik_y)$	$-i\sqrt{\frac{2}{3}}\pi\frac{\partial}{\partial z}$	N^*	$-M$	0	G

where the label Γ specifies the irreducible representation of the T_d double group; $|s\rangle$ represents the s-like spatial function, and $|x\rangle$, $|y\rangle$, and $|z\rangle$ represent the p-like functions; and the arrows designate the two eigenspinors of the operator σ_z:

$$\uparrow=\begin{pmatrix}1\\0\end{pmatrix} \quad \text{and} \quad \downarrow=\begin{pmatrix}0\\1\end{pmatrix} \tag{A3}$$

The two-band effective mass Hamiltonian can be easily obtained by taking the HH and LH elements in Table 1. The coefficient matrices **S**, **T**, and **U** are also immediately obtained by inspecting the order of derivatives in the table.

The modified Luttinger parameters that enter into the above effective mass Hamiltonian are related to the original Luttinger parameters [39], by

$$\gamma_1=\gamma_1^L-\frac{\mathcal{E}_p}{3\mathcal{E}_g+\Delta},\ \gamma_2=\gamma_2^L-\frac{1}{2}\frac{\mathcal{E}_p}{3\mathcal{E}_g+\Delta},$$
$$\text{and } \gamma_3=\gamma_3^L-\frac{1}{2}\frac{\mathcal{E}_p}{3\mathcal{E}_g+\Delta}, \tag{A4}$$

The values of these parameters used for the present computations are shown in Table 2. Notations associated with band structure are defined in Fig. 8.

The parameter m_0' can be evaluated from the relation of

$$\mathcal{E}_c+\frac{\hbar^2}{2m_0}A'k^2+\frac{\hbar^2k^2}{2m_0}=\mathcal{E}_c+\frac{\hbar^2k^2}{2m_0'}. \tag{A5}$$

Here A' is given by [42]

$$A'=\frac{2}{m_0}\sum_{nj}\frac{|\langle s|p_x|n\Gamma_4\, j\rangle|^2}{\mathcal{E}_c-\mathcal{E}_{n\Gamma_4}}, \tag{A6}$$

where j labels the row to which the function associated with Γ belongs, and n specifies the band (in the summation the bottom

Table 2. Band parameters.

	γ_1^L	γ_2^L	γ_3^L	γ_1	γ_2	γ_3	$\mathcal{E}_g$	$\mathcal{E}_p$	Δ	m_c^*	m_0'
GaAs	6.95[a]	2.25[a]	2.86[a]	1.85[f]	−0.3[f]	0.31[f]	1.52[a]	25.0[a]	0.34[b]	0.067[a]	4.47[e]
AlAs	4.04[c]	0.78[c]	1.57[c]				3.13[a]	21.1[c]	0.30[b]	0.150[b]	
AlGaAs	6.03[d]	1.79[d]	2.45[d]	2.12[f]	−0.17[f]	0.5[f]	1.92[b]	23.8[d]	0.327[b]	0.093[b]	2.26[e]

[a] Ref. [40]. [b] Ref. [33].[c] Ref. [41].[d] Calculated by a linear interpolation.
[e] Obtained by fitting. [f] Calculated by (A4).

of conduction band is not included because this band is included in the primary band set). Thus we have

$$\frac{m_0}{m_0'} = A' + 1. \tag{A7}$$

As most of contribution to A' comes from the interaction between $\mathcal{E}_c - \mathcal{E}'$, A' can be calculated approximately, once $\widetilde{\mathcal{E}_p}$ is known, with

$$A' \cong \frac{\widetilde{\mathcal{E}_p}}{\mathcal{E}_c - \mathcal{E}_c'}, \tag{A8}$$

where

$$\widetilde{\mathcal{E}_p} = \frac{2}{m_0} |\langle s|p_x|\mathcal{E}_c'\Gamma_4\, j\rangle|^2. \tag{A9}$$

On the other hand, the parameter m_0' can be evaluated by another way [38]

$$\frac{1}{m_c^*} \approx \frac{1}{m_0} + \frac{2p_0^2}{3\hbar^2}\left(\frac{2}{\mathcal{E}_g} + \frac{1}{\mathcal{E}_g + \Delta}\right), \tag{A10}$$

where

$$P_0 = \frac{\hbar}{m_0}\langle s|p_x|\Gamma_4\, j\rangle, \tag{A11}$$

with P_0 being obtained by a different method. However, since uncertainty in the input parameters for the calculation can cause a large fluctuation in the evaluation of m_0', we determine this parameter empirically by fitting the lowest CB subband energy to that obtained based on the single-band effective-mass equation with effective mass of $m_c^* = 0.0067$ (Table 2).

REFERENCES

[1] S. Mori and T. Ando, "Intersubband Scattering Effect on the Mobility of a Si (100) Inversion Layer at Low Temperatures," *Phys. Rev. B*, Vol. 19, No. 12, 1979, pp. 6433−6441.

[2] T. Ando and S. Mori, "Electronic Properties of a Semiconductor Superlattices I," *J. Phys. Soc. Jpn.*, Vol. 47, No. 5, 1979, p. 1518−1527; S. Mori and T. Ando, "Electronic Properties of a Semiconductor Superlattices II," *J. Phys. Soc. Jpn.*, Vol. 48, No. 3, 1980, pp. 865−873.

[3] M. Altarelli,"Electronic Structure and Semiconductor-Semimetal Transition in InAs-GaSb Superlattices," *Phys. Rev. B*, Vol. 28, No. 2, 1983, pp. 842−845.

[4] G. Bastard, "Quantum-Size Effects in the Continuum States of Semiconductor Quantum Wells," *Phys. Rev. B*, Vol. 30, No. 6, 1984, pp. 3547−3549.

[5] W. Potz, W. Porod, and D.K. Ferry, "Theoretical Study of Subband Levels in Semiconductor Heterostructures," *Phys. Rev. B*, Vol. 32, No. 6, 1985, pp. 3868−3875.

[6] G. Bastard and J.A. Brum, "Electronic States in Semiconductor Heterostructures," *IEEE J. Quantum Electronics*, Vol. QE-22, No. 9, 1986, pp. 1625−1644.

[7] M.V. Klein, "Phonons in Semiconductor Superlattices," *IEEE J. Quantum Electronics*, Vol. QE-22, No. 9, 1986, pp. 1760−1770.

[8] L. Esaki, "A Bird's-Eye View on the Evolution of Semiconductor Superlattices and Quantum Wells," *IEEE J. Quantum Electronics*, Vol. QE-22, No. 9, 1986, pp. 1611−1624.

[9] D.L. Smith and C. Mailhiot, "k.p Theory of Semiconductor Superlattice Electronic Structure. I. Formal Results," *Phys. Rev. B*, Vol. 33, No. 12, 1986, pp. 8345−8359; C. Mailhiot and D.L. Smith, "k.p Theory of Semiconductor Superlattice Electronic Structure. II. Application to Ga1-xInxAs-Al1-yInyAs [100] Superlattices," *Phys. Rev. B*, Vol. 33, No. 12, 1986, pp. 8360−8372.

[10] S. Fraizzoli and F. Bassani, "Shallow Donor Impurities in GaAs-Ga1-xAlxAs Quantum Well Structures: Role of the Dielectric-Constant Mismatch," *Phys. Rev. B*, Vol. 41, No. 8, 1990, pp. 5096−5103.

[11] N.F. Johnson, H. Ehrenreich, P.M. Hui, and P.M. Young, "Electronic and Optical Properties of III-V and II-VI Semiconductor Superlattices," *Phys. Rev. B*, Vol. 41, No. 6, 1990, pp. 3655−3669.

[12] H. Xie, L.R. Fiedman, and L.R. Ram-Mohan, "Nonlinear Optical Properties of GaAs/$Ga_{1-x}Al_x$ As Superlattices," *Phys. Rev. B*, Vol. 42, No. 11, 1990, pp. 7124−7131.

[13] J.B. Xia, S.F. Ren, and Y.C. Chang, "Electronic Structures of GdAs/GaAs Superlattices," *Phys. Rev. B*, Vol. 43, No. 2, 1991, pp. 1692−1698.

[14] L.H. Peng and C.G. Fonstad, "Multiband Coupling Effects on Electron Quantum Well Intersubband Transitions," *J. Appl. Phys.*, Vol. 77, No. 2, 1995, pp. 747−754.

[15] J.N. Schulman and Y.-C. Chang, *Phys. Rev. B*, Vol. 33, No. 4, 1986, pp. 2594−2601; see also the Refs. 1−7 included in Ref. 17.

[16] G. Bastard, "Superlattice Band Structure in the Envelope-Function Approximation," *Phys. Rev. B*, Vol. 24, No. 10, 1981, pp. 5693−5697; "Theoretical Investigations of Superlattice Band Structure in the Envelope-Function Approximation," *Phys. Rev. B*, Vol. 25, No. 12, 1982, pp. 7584−7597, see also the Refs. 11−15 included in Ref. 17.

[17] L.R. Ram-Mohan, K.H. Yoo, and R.L. Aggarwal, "Transfer-Matrix Algorithm for the Calculation of the Band Structure of Semiconductor Superlattices," *Phys. Rev. B*, Vol. 38, No. 9, 1988, pp. 6151−6159.

[18] B. Jonsson and S.T. Eng, "Solving the Schrodinger Equation in Arbitrary Quantum-Well Potential Profiles Using the Transfer Matrix Method," *IEEE J. Quantum Electronics*, Vol. QE- 26, No. 11, 1990, pp. 2025−2035.

[19] S.L. Chuang, "Efficient Band-Structure Calculations of Strained Quantum Wells," *Phys. Rev. B*, Vol. 43, No. 12, 1991, pp. 9649−9661.

[20] H. Schlosser and N.O. Lipari, *Phys. Rev. B*, Vol. 8, 1973, p. 2697.

[21] M. Altarelli, "Electronic Structure and Semiconductor-Semimetal Transition in InAs-GaSb Superlattices," *Phys. Rev. B*, Vol. 28, No. 2, 1983, pp. 842−845.

[22] D.A. Broido and L.J. Sham, "Effective Masses of Holes at GaAs-AlGaAs Heterojunctions," *Phys. Rev. B*, Vol. 31, No. 2, 1985, pp. 888−892.

[23] M. Altarelli, U. Ekenberg, and A. Fasolino, "Calculations of Hole Subbands in Semiconductor Quantum Wells and Superlattices," *Phys. Rev. B*, Vol. 32, No. 8, 1985, pp. 5138−5143.

[24] D. Ahn and S.L. Chuang, "Exact Calculations of Quasibound States of an Isolated Quantum Well with Uniform Electric Field: Quantum-Well Stark Resonance," *Appl. Phys. Lett.*, Vol. 49, No. 1, 1986, pp. 1450−1453.

[25] A. Twardoski and C. Hermann, "Variational Calculation of Polarization of Quantum-Well Photoluminescence," *Phys. rev. B,* Vol. 35, No. 15, 1987, pp. 8144−8153.

[26] L.C. Andreani, A. Pasquarello, and F. Bassani, "Hole Subbands in Strained GaAs-$Ga_{1-x}Al_xAs$ Quantum Wells: Exact Solution of the Effective-Mass Equation," *Phys. Rev. B*, Vol. 36, No. 11, 1987, pp. 5887−5894.

[27] G.C. Wetsel, Jr., "Calculation of the Energy-Band Structure of the Kronig-Penney Model Using the Nearly-Free and Tightly-Bound-Electron Approximations," *Am. J. Phys.*, Vol. 46, No. 7, 1978, pp. 714−720.

[28] H.S. Cho and R. Prucnal, "New Formalism of the Kronig-Penney Model with Application to Superlattices," *Phys. Rev. B*, Vol. 36, No. 6, 1987, pp. 3237−3242.

[29] G.T. Zimanyi, K. Vladar, and A. Zawadowski, "Path-Integral Method for a Heavy Particle Moving in a Periodic Potential and Screened by a Light Degenerate Fermi Gas," *Phys. Rev. B*, Vol. 36, No. 6, 1987, pp. 3186−3198.

[30] B. Chen, M. Lazzouni, and L.R. Ram-Mohan, "Diagonal Representation for the Transfer- Matrix Method for Obtaining Electronic Energy Levels in Layered Semiconductor Heterostructures," *Phys. Rev. B*, Vol. 45, No. 3, 1992, pp. 1204−1212.

[31] E.O. Kane, *Semiconductors and Semimetals*, Vol. 1, R.K.Willadson and A.C. Beer, ed., Academic, New York, 1966.

[32] S. Gasiorowicz, *Quantum Physics*, John Wiley & Sons, 1974.

[33] *Key Parameters in Physics: Gallium Asenide*, No. 1, J.S. Blakemore, ed., American Institute of Physics, New York, 1987.

[34] B.W. Kim and A. Majerfeld, "Electronic and Intersubband Optical Properties of p-Type GaAs/AlGaAs Superlattices for Infrared Photodetectors," *J. Appl. Phys.*, Vol. 77, No. 9, 1995, pp. 4552−4558.

[35] Z. Ikonic, V. Milanovic, D. Tjapkin, and S. Pajevic, "Effective-Mass-Mismatch-Induced Intersubband Absorption Line Broadening in Semiconductor Quantum Wells," *Phys. Rev. B*, Vol. 37, No. 6, 1988, pp. 3097−3100.

[36] D.M. Szmyd, M.C. Hanna, A. Majerfeld, "Heavily Doped GaAs: Se. II. Electron Mobility," *J. Appl. Phys.*, Vol. 68, No. 5, 1990, pp. 2376−2381.

[37] M. Zaluzny, "Intersubband Absorption Line Broadening in Semiconductor Quantum Wells: Nonparabolicity Contribution," *Phys. Rev. B*, Vol. 43, No. 5, 1991, pp. 4511−4514.

[38] *Quantum Phenomena, Modular Series on Solid State Devices*, Volume VIII, S. Datta, ed., Addison-Wesley Publishing Company, Inc., 1989.

[39] J.M. Luttinger, "Quantum Theory of Cyclotron Resonance in Semiconductors: General Theory," *Phys. Rev.*, Vol. 102, No. 4, 1956, pp. 1030−1041.

[40] "Numerical Data and Functional Relationships in Science and Technology," *Semiconductors*, Vol. 22, O. Madelung, ed., Springer-Verlag, 1987.

[41] P. Lawaetz, "Valence-Band Parameters in Cubic Semiconductors," *Phys. Rev. B*, Vol. 4, No. 10, 1971, pp. 3460−3467.

[42] T.B. Bahder, "Eight-Band k.p Model of Strained Zinc-Blende Crystals," *Phys. Rev. B*, Vol. 41, No. 17, 1990, pp. 11992−12001.

Byoung-Whi Kim received the Ph. D. degree in electrical and computer engineering from University of Colorado, Boulder, Colorado in 1993. From 1983 to 1988, he was involved in the development of a digital switching system in ETRI. Since he joined ETRI again in 1994, he has been working on III-V compound-semiconductor optical switches based on strain-induced piezoelectric effects. His research interests include theoretical physics of compound semiconductor materials and optoelectronic devices.

Yong Il Jun received the B.S. in electrical engineering from Korea University in 1981 and the M.S. in electrical engineering in KAIST in 1983. From 1983 to 1987, He was a researcher at Gold Star Precision and developed a front end X-band receiver, and an antenna of direction finder. Since 1987, he has been a senior engineer of ETRI, and develops MMIC, U-interface PHY-layer protocol engine, and ATM switching chipsets. His current research areas are switching element, switching fabric, traffic control, and signal integrity of large-scale system.

Hee Bum Jung received the B.S. degree in electronics engineering from Sogang University, Seoul, Korea in 1981, the M.S. degree in electrical engineering from Korea Advanced Institute of Science and Technology in 1983, and the Ph.D. degree in electrical engineering from Columbia University, New York, New York, U.S.A. in 1992. From 1983 to 1987 he was with KIET (former ETRI), Gumi, Korea, where he was involved in the development of custom integrated circuit design and modeling. While in Columbia University, he was also a student intern (1990 to 1991) of AT&T Bell Laboratory, Murray Hill, NJ, U.S.A. with research topic of HBT modeling. He rejoined ETRI in 1993 to pursue VLSI circuit design. His interests include analog-digital mixed signal VLSI design, circuit modeling, and CMOS RF & analog front-end IC's for IMT-2000 terminal equipments.